Wnt-dependent assembly of supermolecular Dishevelled-3-based complexes

Noriko Yokoyama[1,*], Urszula Golebiewska[2], Hsien-yu Wang[2] and Craig C. Malbon[1]

[1]Department of Pharmacology and [2]Department of Physiology and Biophysics, Health Sciences Center, State University of New York at Stony Brook, Stony Brook, NY 11794-8651, USA

*Author for correspondence (noriko@pharm.stonybrook.edu)

Accepted 22 July 2010
Journal of Cell Science 123, 3693-3702

doi:10.1242/jcs.075275

Summary

Dishevelled-3 (Dvl3) is a multivalent scaffold protein that is essential to Wnt signaling during development. Although Dvl-based punctae have been visualized by fluorescence microscopy; the physical nature and dynamic character of the such complexes are enigmatic. We use steric-exclusion chromatography, affinity pull-downs, proteomics and fluorescence correlation microscopy to characterize supermolecular Dvl3-based complexes of totipotent mouse F9 cells. The molecular mass of the complexes ranges from that of homodimeric Dvl3 to well-defined peaks harboring supermolecular complexes of 0.4 to 2.0 MDa. Addition of Wnt3a stimulates the formation of Dvl3-based complexes of greater molecular mass within 30 minutes. The presence of DKK1 and knockdown of Dishevelled proteins block formation of the 2 MDa Dvl3-based complexes and also block Wnt3a stimulation of the canonical pathway. Fluorescent correlation microscopy identified supermolecular Dvl3-based complexes with a molecular mass >30 MDa in live cells; these complexes were provoked to form structures with even greater molecular mass by Wnt3a. We establish for the first time the physical and functional nature of very large, supermolecular Dvl3-based complexes.

Key words: Dishevelled, Oligomerization, Supermolecular, Complexes, Wnt3a

Introduction

Wnt signaling regulates numerous cellular pathways, including embryonic development and adult tissue homeostasis (Nusse, 2005; Wodarz and Nusse, 1998; Clevers, 2006; Glass and Karsenty, 2006; Wang and Wynshaw-Boris, 2004). Wnt signaling branches into at least three distinct pathways: canonical, non-canonical and planar cell polarity (PCP) (Liu et al., 2001; Willert et al., 2003; He et al., 2004; Wallingford and Habas, 2005; Katanaev et al., 2005; Malbon, 2005). Dishevelled (Dsh/Dvl) is the essential component for all three pathways. It is considered that Dvl functions as a scaffold protein that bridges the receptors and distinct downstream signaling components.

Wnt proteins are secreted glycoproteins that bind to members of the Frizzled (Fz) family of G-protein-coupled receptors and to co-receptor low density lipoprotein receptor-related protein LRP5 and LRP6 (LRP5/6). Binding of Wnt3a to the extracellular domain of Frizzled-1 (Fz1) and co-receptor LRP5/6 facilitates the phosphorylation of LRP5/6 by glycogen synthase kinase-3β (GSK3β). This triggers the interaction of Fz–LRP5/6 complex with dynamic multiprotein complexes, including adenomatous polyposis coli (APC), Dvl, Axin, GSK3β and casein kinase 1α (Hart et al., 1998; Kishida et al., 1998). Dvl is a scaffold protein that facilitates destruction of multiprotein complexes (Hart et al., 1998; Kishida et al., 1998; Malbon, 2005). As a result, stabilized β-catenin translocates to the nucleus and enhances Lef/Tcf transcription (Clevers, 2006; Angers and Moon, 2009; van Amerongen and Nusse, 2009). Misregulation of β-catenin phosphorylation and degradation is the hallmark of several cancers and other diseases.

Upstream signaling pathways that regulate inhibition of GSK3β activity still remain to be determined. *Xenopus* Dsh is associated with vesicle-like organelles that are directionally transported to the prospective dorsal side of the embryo (Miller et al., 1999). Dvl proteins are thought to oligomerize and they occur in 'punctate' structures when probed using autofluorescently tagged Dvl fusion proteins (Axelrod et al., 1998; Kishida et al., 1999; Rothbacher et al., 2000). Properties of dynamic polymerization viewed by optical means correlate with the activation of Wnt/β-catenin signaling (Schwarz-Romond et al., 2007a; Schwarz-Romond et al., 2007b). Wnt likewise induces LRP6 aggregation and phosphorylation in a Dvl-dependent manner. Dvl mutants that appear to lack normal oligomerization also influence the formation of LRP6 complexes (Bilic et al., 2007).

Fly Dsh and three isoforms of mammals Dvl proteins (Dvl1–Dvl3) all share several prominent, highly conserved domains: a Dsh-homology domain called DIX; a conserved sequence element with homology to the postsynaptic density protein PSD-95, Discs-large, and ZO-1, termed PDZ; and a Dvl, Egl-10, pleckstrin domain, termed DEP (Wharton, 2003). Dvl is believed to be recruited through its PDZ domain (Wong et al., 2003). The DIX domain is crucial for the ability of Dvl to recruit Axin and for DIX-dependent dynamic self-association of Dvl2 (Schwarz-Romond et al., 2007a; Schwarz-Romond et al., 2007b).

Previous studies reveal distinct localization of Dvl isoforms in mouse F9 teratocarcinoma cells (F9) (Yokoyama et al., 2007). Dvl3 has a role in Wnt/β-catenin signaling that is distinct from those of the more abundant Dvl1 or Dvl2 (Yokoyama et al., 2007). Wnt stimulation of the canonical pathway stimulates trafficking of Dvl proteins and other molecules that are crucial to the pathway (Yokoyama et al., 2007). Here, we exploit the size-exclusion chromatography technique [with the capacity to resolve complexes with molecular mass from 50 kDa to 2 MDa], affinity pull-downs, proteomics and fluorescence correlation microscopy (FCS) to identify and probe supermolecular Dvl3-based assemblies formed

in response to Wnt3a. The size and composition of Dvl3-based complexes is shown to be temporally sensitive to Wnt3a. This study, the first temporal-spatial analysis of Dvl3-based complexes, reveals a complex, dynamic association of molecules that are central to Wnt/β-catenin canonical signaling.

Results

Formation of supermolecular complexes of Dvl

We analyzed the ability of Dvl2, the most abundant isoform in mammalian cells (Lee et al., 2008), to form complexes. Dvl2 was first isolated from whole-cell lysates prepared from totipotent mouse F9 embryonic teratocarcinoma (F9) cells and subjected to pull-downs with anti-Dvl2 antibody. Dvl2 was resolved by SDS-PAGE, analyzed and protein stained (Fig. 1A). Based on primary sequence only, the mass for Dvl proteins, ranged from 78.1 kDa (Dvl3) to 78.9 kDa (Dvl2). The appearance of Dvl2 with a molecular mass of ~250 kDa and little monomeric form suggests the formation of Dvl-based supermolecular complexes. The nature of the 250 kDa form of Dvl was probed by PAGE in SDS (Fig. 1B, left) versus 8 M urea (Fig. 1B, right), a strong chaotropic agent that is capable of disrupting most intermolecular interactions. In the presence of 8 M urea, Dvl2 migrated as a two species (65 kDa and 70 kDa), stained positively in immunoblots (Fig. 1B, right). Proteomic analysis showed the Dvl2 complexes were either homodimeric Dvl proteins or heterodimeric with another poorly staining molecular partner. Because mammalian Dvl proteins display a DIX domain, formation of either homodimeric or heterodimeric) complexes (with other molecules such as Axin that harbor a DIX domain) might be expected. Immunofluorescence images of Dvl2 in Wnt-treated cells have been interpreted as the formation of membrane-associated protein 'aggregates' in response to Wnt (Bilic et al., 2007). The amount of homodimeric or heterodimeric, SDS-resistant forms of Dvl2 was not influenced by treatment of cells with Wnt3a for 30 minutes (Fig. 1).

High-performance size-exclusion analysis of Dvl-based supermolecular complexes

The visualization of large punctate assemblies by fluorescence microscopy prompted our search for supermolecular forms of mammalian Dvl proteins. Cell extracts were prepared and subjected to size-exclusion column chromatography (HiLoad Superdex^{TM} 200 prep grade 26/60, fast-performance AKTA liquid chromatography). To obtain a suitable performance, a high-pressure column, 60 cm in length, was engineered to permit high resolution over a size range of 43 kDa to ~2.0 MDa. Molecular standards displayed excellent and highly reproducible peak separation over this range (Fig. 1C). Dvl1, Dvl2 or Dvl3-based supermolecular complexes were resolved and individual fractions subjected to SDS-PAGE and analyzed by immunoblotting with isoform-specific antibodies (Fig. 2). Dvl2, the isoform that constitutes >90% of cellular pool of Dvl, displayed three major peaks: two large peaks (one with a peak mass of ~1.6 MDa, the other centered about 0.5 MDa), and a minor peak (~80 kDa), which is probably monomeric Dvl2 (Fig. 2A). The 1.6 MDa peak of Dvl2 displayed the same higher-complexity immunostaining (Fig. 1). The hydrodynamic behavior of these peaks was highly reproducible and was unaffected by the absence or presence of subcritical micelle concentrations of non-ionic detergents used in the lysis buffer (data not shown). Staining for Dvl1 revealed the same two large supermolecular forms observed for Dvl2-based complexes: 1.6 MDa and 0.5 MDa (Fig. 2B). Dvl3-based complexes resolved as a broad peak centered

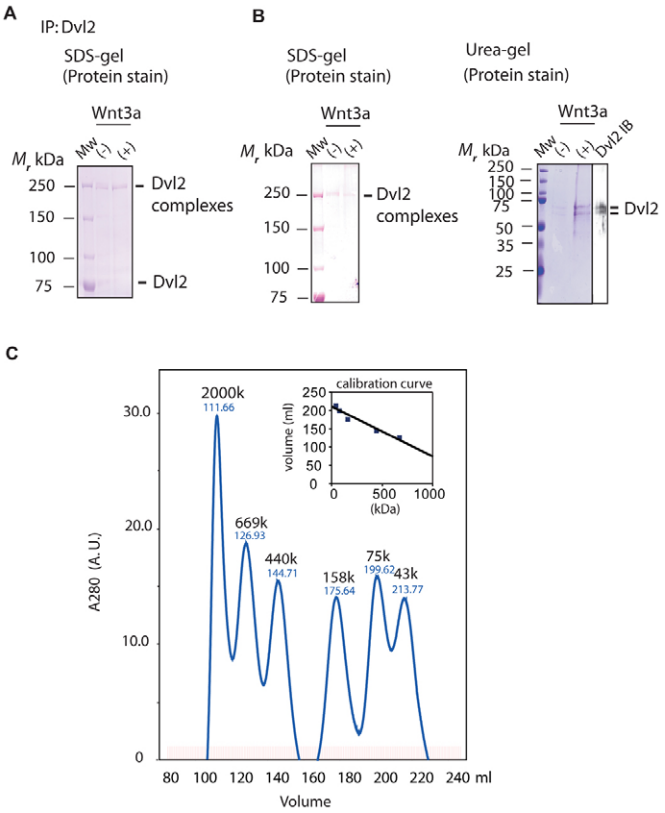

Fig. 1. Formation of large Dvl2-based complexes. (**A**) Dvl2 forms large complexes. Mouse F9 teratocarcinoma cells were stimulated with or without Wnt3a for 30 minutes. Cell lysates were subjected to immunoprecipitation with anti-Dvl2 antibody. Bound proteins were analyzed by SDS-PAGE and visualized with Coomassie Brilliant Blue. The results shown are representative of five independent experiments. (**B**) Dvl2 complexes migrate differently in the presence of SDS or 8 M urea. High molecular mass bands (~250 kDa) were excised from the gels, and the proteins were extracted. Extracted proteins were analyzed by PAGE either in the presence of SDS (left) or 8 M urea (right). Proteins are stained with Coomassie Brilliant Blue. Small portion of the extracted samples was analyzed by SDS-PAGE in the presence of urea and immunoblotting with anti-Dvl2 antibody (right). Representative gels from five independent experiments are shown. (**C**) Resolution of Superdex 200 column. Mixtures of molecular marker proteins (Blue Dextran 2000, thyroglobulin, ferritin, aldolase, conalbumin and ovalbumin) were applied to a Superdex 200 column, which was pre-equilibrated with 20 mM Tris-HCl, pH 8.0, 0.2 M NaCl and 10% glycerol. Elution profile was monitored by absorbance at 280 nm.

at ~210 kDa, as well as the 0.8–2.2 MDa complexes (Fig. 2A,B,C). Dvl3 and Dvl1-staining of the lower end of the chromatogram displayed little monomeric Dvl (Fig. 2B,C). The presence of GSK3β and Axin, key molecules in Wnt/β-catenin canonical signaling complexes, was also analyzed by immunostaining. GSK3β (46.7 kDa) was distributed widely, was dominant in the 40–160 kDa region, yet was clearly present both in the larger 0.5 and ~1.6 MDa regions (Fig. 2D). Axin was detected in the 0.5–0.7 MDa regions, in which GSK3β, Dvl1 and Dvl2 were found.

Wnt3a stimulates formation of dynamic supermolecular Dvl-based complexes

The major peak of the Dvl3-based complex migrated as a broad peak, with a range of ~130–140 kDa (centered at ~210 kDa) to

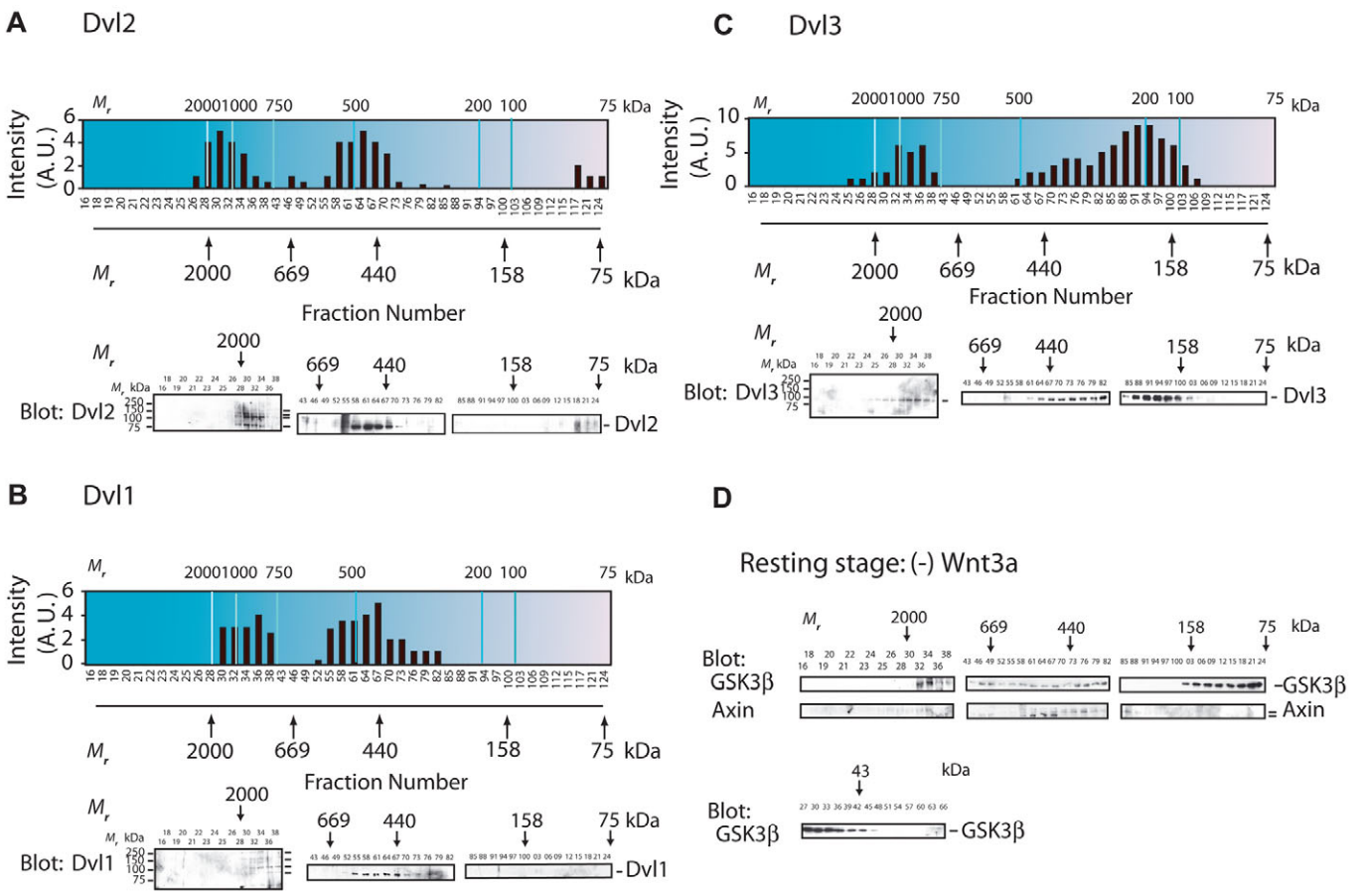

Fig. 2. Dvl proteins form distinct large-scale complexes in resting cells. Rfz1-expressing F9 cells were disrupted by passage through a 23-gauge needle. Cell lysates were centrifuged at 20,000 ***g*** for 10 minutes. Supernatants were filtered (0.45 μm) and then diluted in buffer with no detergent. The fractions (20 mg protein) were applied to Superdex 200 column (AKTA, GE HealthCare). Proteins were analyzed by SDS-PAGE and western immunoblotting with Dvl-isoform-specific antibodies (bottom). Blots were quantified by the calibrated scanner (top). The calculated, relative molecular mass positions from calibration curve are labeled at the top. The bottom numbers indicate fraction numbers. Arrows indicate the precise position at which calibration proteins elute from Superdex 200. (**A**) Dvl2-based complexes at the resting stage. (**B**) Dvl1-based complexes at the resting stage. (**C**) Dvl3-based complexes at the resting stage. (**D**) GSK3β and Axin distribution at the resting stage. Fractions were subjected to SDS-PAGE and analyzed by immunoblotting with either anti-GSK3β or anti-Axin antibody. Representative blots of at least two separate experiments are displayed.

tailing complexes of ~500 kDa. We probed whether treating cells with Wnt3a altered the size of the Dvl3-based complexes. The 75–750 kDa region of the chromatogram revealed Wnt3a-stimulated changes in the migration of the Dvl3-based complexes (Fig. 3A). At 30 minutes after addition of Wnt3a, a sharpening of the major peak was clear, which progressed until 1 hour, when a new peak of slower mobility (550–750 kDa) was first observed. For Dvl-2- and Dvl-1-based complexes, Wnt3a treatment provoked a broadening of the >500 kDa peaks to generally higher molecular masses (Fig. 3B,C; supplementary material Fig. S1).

Chromatograms of 0.75 to 2.0+ MDa (i.e. the highest mass resolution of HiLoad® Superdex® 200 prep-grade 26/60 matrix) Dvl3-based supermolecular complexes formed in response to Wnt3a stimulation were remarkable (Fig. 3C). Within 1 hour, Wnt3a treatment of the cells provoked a progressive increase in the apparent mass of Dvl3-based complexes. These Wnt3a-stimulated supermolecular Dvl3-based complexes were very large (≥2.0 MDa). The abundance of very large supermolecular complexes increased in the first hour, reverting to 1–2 MDa within the next hour (Fig. 3C). In response to Wnt3a stimulation, Dvl2-based complexes displayed increased apparent masses, although none of these complexes approached the limit size of those formed by Dvl3-based complexes (Fig. 3D). Complexes including Dvl1, by contrast, displayed little change in size in response to Wnt3a (Fig. 3D). Using a matrix designed to resolve at very highest mass ranges (limit resolution of 10 MDa), we were able to establish conclusively that the peak of the Dvl3-based supermolecular complex (separated by steric-exclusion chromatography) was in fact 2.0 MDa (Fig. 3E).

GSK3β and Axin also migrated with supermolecular complexes of increasing apparent mass (>1.0 MDa) in response to Wnt3a stimulation for 30 minutes (Fig. 4A,B). The amount of Axin associated with the 1.0+ MDa species increased over 30–60 minutes of exposure of Wnt3a. The similarities of the migration of GSK3β, Axin, and Dvl3 in supermolecular complexes (~2 MDa) were evident by 30 minutes (Fig. 4A,B and supplementary material Fig. S2A), but not later (supplementary material Fig. S2A,B), suggesting that GSK3β and Axin co-migrate with the Dvl3 upon 30 minutes activation of the Wnt/β-catenin canonical pathway by Wnt3a. At 30 minutes after Wnt3a treatment, Dvl2 and Axin likewise appeared to co-migrate with ~2 MDa for up to 2 hours after addition of Wnt3a (supplementary material Fig. S2C). Wnt3a provoked a

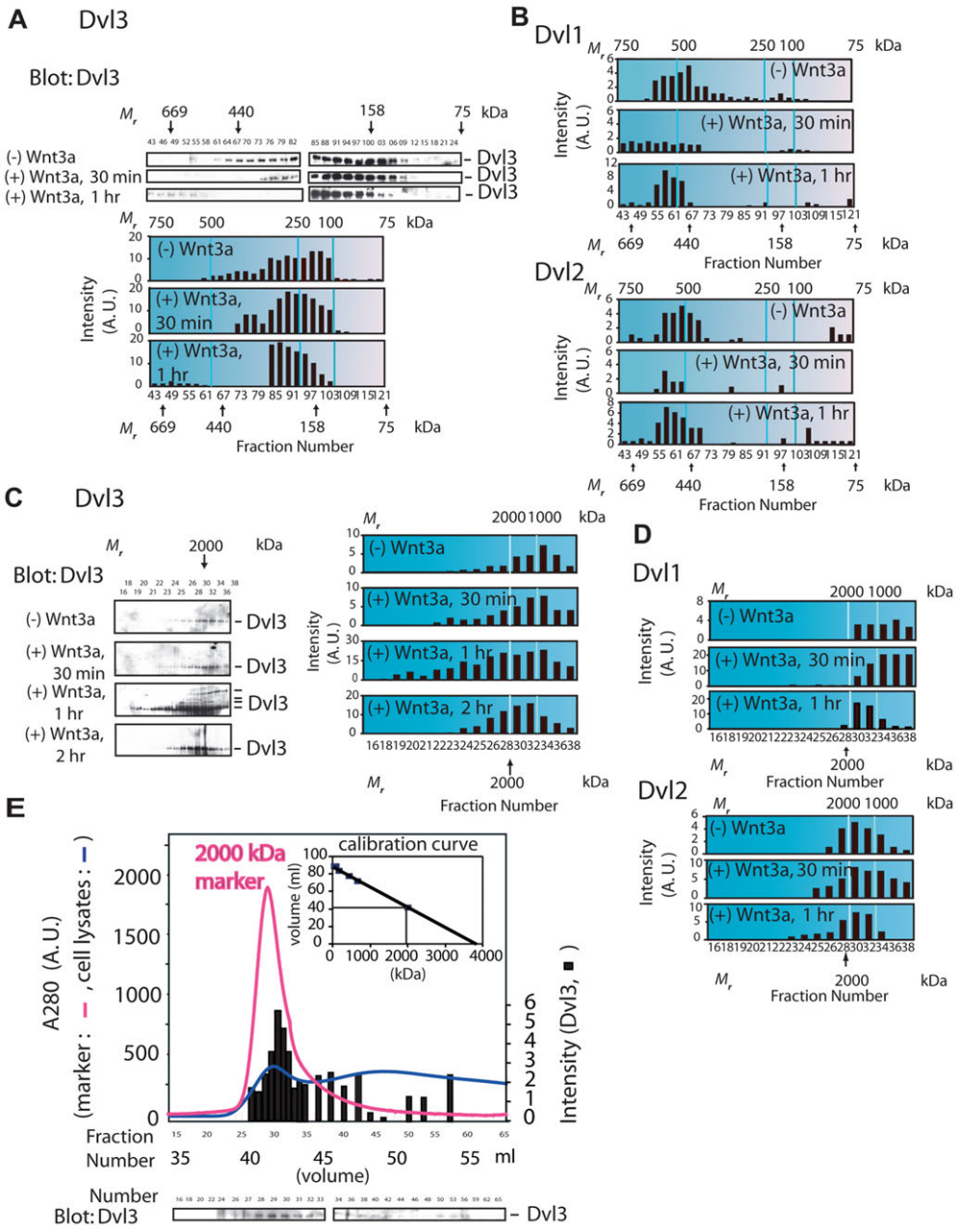

Fig. 3. Dvl proteins form supermolecular multiprotein complexes in response to Wnt3a in a time-dependent manner. Dvl proteins assemble supermolecular complexes in response to Wnt3a. F9 cells were stimulated with Wnt3a for the indicated times. Cells were lysed and filtered supernatants were subject to steric exclusion chromatography on Superdex 200. Fractions were analyzed by SDS-PAGE and resolved proteins immunoblotted with isoform-specific Dvl antibodies. Blots were quantified with the calibrated scanner. (**A**) Dvl3 blot (top) and quantitative analysis of the 75–750 kDa regions (bottom). (**B**) Quantitative analysis of Dvl1 (top) and Dvl2 (bottom) in region 75–750 kDa. (**C**) Dvl3 blot (left) and quantitative analysis of Dvl3 (right) in region above 750 kDa. (**D**) Quantitative analysis of Dvl1 and Dvl2 in region above 750 kDa. Results are representative of at least two independent experiments. (**E**) Determination of molecular mass of supermolecular Dvl3-based complexes. F9 cells were stimulated with Wnt3a (20 ng/ml) for 1 hour. Cell extracts were prepared and applied to a Sephacryl S-400 column (HiPrep Sephacryl S400 high-resolution column 16/60, fast-performance AKTA liquid chromatography). Fractions (0.45 ml) were collected and analyzed by SDS-PAGE and the resolved proteins immunoblotted with anti-Dvl3 antibody. Pink and blue lines show the elution pattern of Blue Dextran (marker protein, 2000 kDa) and cell lysates, respectively. Filled bars display relative Dvl3 content in each fraction. Bottom panel shows blot with anti-Dvl3 antibody. Blots were scanned by calibrated scanner and displayed in the top panel.

transient formation of Axin-enriched, Dvl-based complexes with ~0.6 MDa (supplementary material Fig. S2D). We further probed these molecules in the ~2 MDa complexes using Dvl3-based pull downs. At 30 minutes, Dvl3 assembled in complexes with Dvl1, Dvl2, Axin and GSK3β (supplementary material Fig. S2E), as well as with a significant number of other proteins visualized by silver staining (supplementary material Fig. S2F). This level of complexity would be predicted, based upon known and suspected protein partners operating in the Dvl-based signaling of Wnt3a (see http://www.stanford.edu/~rnusse/wntwindow.html). LRP6 was present in ~2 MDa complexes in the absence of Wnt stimulation. Migration of LRP6 in ~2 MDa supermolecular complexes was seen 30 minutes after stimulation, which thereafter reduced within 1 hour of stimulation (supplementary material Fig. S2G). This internalization of LRP6 in response to Wnt3a appears to agree well with observations reported earlier (Yamamoto et al., 2006). The presence of LRP6 in ~2 MDa complexes supports the notion of LRP6 aggregation in a Dvl-dependent manner and the signalosome. Formation of supermolecular Dvl3-based complexes was also detected in response to Wnt3a in HEK293 cells (supplementary material Fig. S2H). HEK293 cells were selected for this study because of their similar profile of expression for Dvl1, Dvl2 and Dvl3 (Lee et al., 2008).

DKK1 blocks both activation of Wnt canonical pathway and formation of supermolecular Dvl3-based complexes

Having demonstrated that the ~2.0 MDa Dvl3-based complexes include key molecules known to participate in the Wnt/β-catenin–Lef-Tcf-sensitive transcriptional response and display dynamic changes in size in response to Wnt3a, we sought to probe the linkage between complex formation and functional output of the pathway. Dickkopf homologue 1 (DKK1) is a well known Wnt

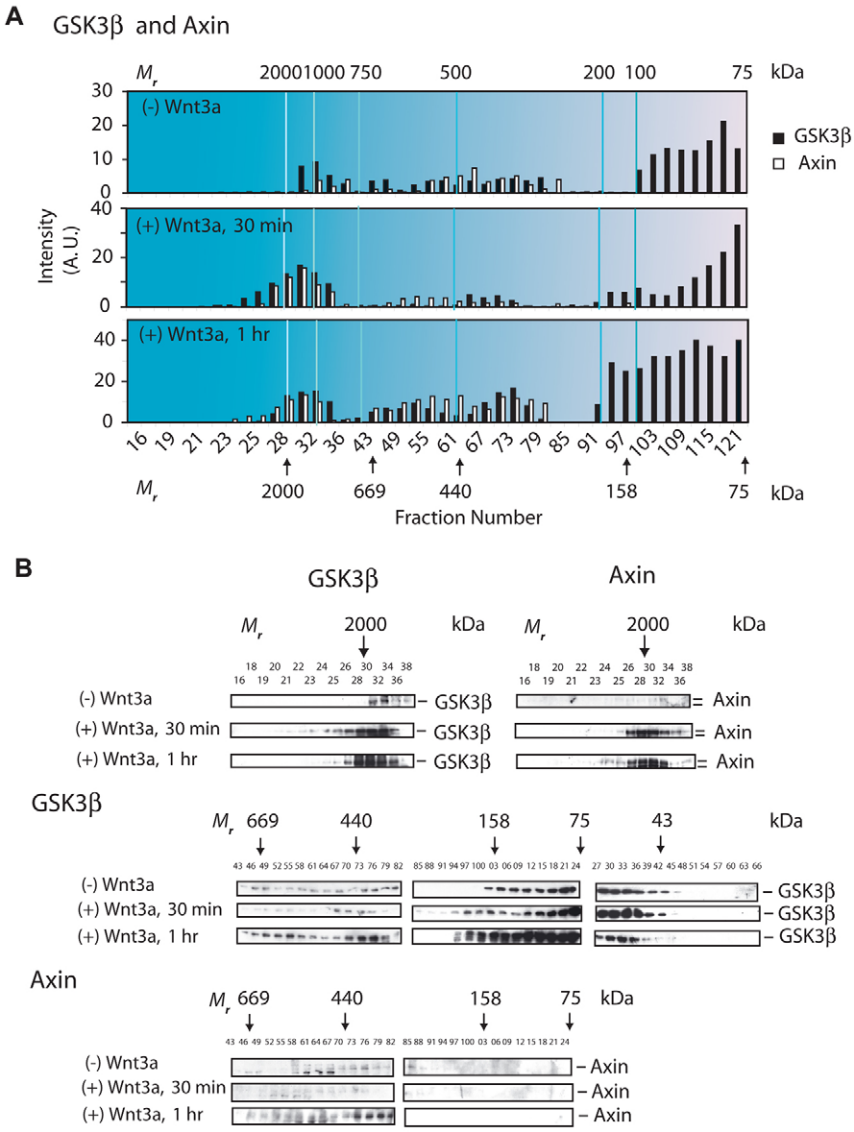

Fig. 4. Co-migration of GSK3β and Axin in response to Wnt3a. (**A**,**B**) Wnt- and time-dependent comigration of GSK3β and Axin. F9 cells expressing Rfz1 were either untreated or treated with Wnt3a for the indicated times. Cell lysates (20 mg protein) were fractionated by Superdex 200 gel filtration column. Proteins were resolved by SDS-PAGE and the resolved proteins immunoblotted, and visualized by staining with either anti-GSK3β antibody or anti-Axin antibody. Relative abundance of Axin and GSK3β was established. Quantitative analysis of GSK3β (filled bars) and Axin (open bars) is displayed in A. Blots are shown in B. Results are from at least two independent experiments.

antagonist that activates the Lef/Tcf-sensitive transcriptional response of Wnt (Nusse, 2001). Treatment of cells with DKK1 for 60 minutes effectively blocked the ability of Wnt3a to stimulate the Lef/Tcf-sensitive response (data not shown), as well as the formation of the very large (>2.0 MDa) supermolecular Dvl3-based complexes provoked in response to Wnt3a (Fig. 5A and supplementary material Fig. S3A).

Constitutively active LRP6 promotes formation of supermolecular Dvl3-based complexes

We were intrigued to see whether activation of the Wnt/β-catenin pathway in the absence of Wnt would stimulate the formation of the very large (>2.0 MDa) supermolecular Dvl3-based complexes. Wnt stimulation can be mimicked by expression of constitutively active mutant (CA-Δ-N)LRP-6 (Tamai et al., 2004). Overexpression of Δ-N-LRP6 in F9 cells stimulated Lef/Tcf transcription in the absence of Wnt3a about fourfold (supplementary material Fig. S3B). Overexpression of CA-Δ-N-LRP6 likewise provoked formation of the very large supermolecular Dvl3-based complexes (Fig. 5B and supplementary material Fig. S3C), similarly to Wnt3a itself.

Overexpression of Dvl1 and Dvl3 activates the canonical pathway of formation of very large Dvl3-based complexes

Exogenous, overexpression of Dvl1 and Dvl3 in mouse F9 cells stimulates the Wnt canonical pathway (Lee et al., 2008). We sought to explore whether activation of the canonical pathway by overexpression of Dvl proteins would provoke the formation of the supermolecular Dvl3-based complexes (Fig. 6A and supplementary material Fig. S4A,B), as was observed in response to Wnt3a (Fig. 2). Overexpression of Dvl1 stimulates both activation of the canonical pathway (data not shown) and an increase in the formation of the very large (>2.0 MDa) supermolecular Dvl3-based complexes (Fig. 6A). Overexpression of Dvl3 provoked a similar activation of Lef/Tcf-sensitive transcription (data not shown) and sharp increase in the formation of very large (>2.0 MDa) Dvl3-based complexes (Fig. 6A). Overexpression of the most abundant Dvl isoform (i.e. Dvl2), by contrast, provoked only a modest Lef/Tcf-sensitive transcriptional response (data not shown) and little formation of the very large (>2.0 MDa) Dvl3-based complexes (Fig. 6A). Thus, the formation of very large, supermolecular Dvl3-based complexes can be specifically mimicked by the overexpression of either Dvl1 or

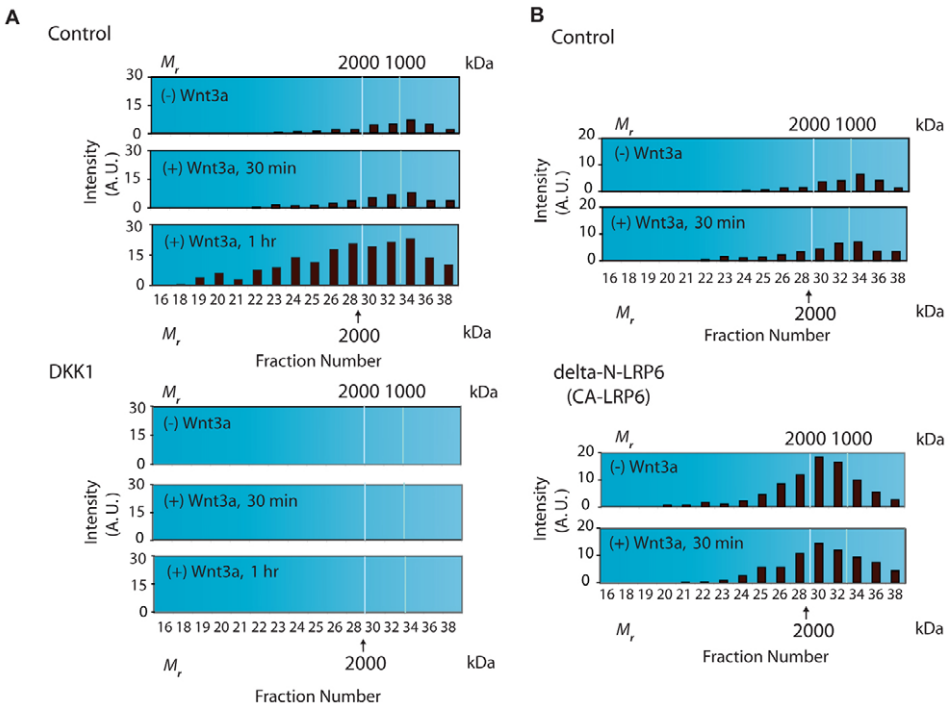

Fig. 5. Blockade of Wnt signaling pathway interrupts formation of supermolecular Dvl3-based complexes, whereas mimicking Wnt signaling enhances formation of supermolecular Dvl3-based complexes. (**A**) Wnt antagonist DKK1 abolishes Dvl3-based supermolecular complexes in response to Wnt3a. F9 cells were either untreated or pretreated with DKK1 (400 ng/ml) for 1 hour, before stimulation with or without Wnt3a (20 ng/ml) for 30 minutes (or 1 hour) in the continued presence or absence of DKK1. Cell extracts were subjected to steric-exclusion chromatography on Superdex 200. Results displayed are representative of at least two independent experiments. (**B**) Expression of constitutively active LRP6 provokes formation of supermolecular Dvl3-based complexes. F9 cells were cotransfected with Rfz1 and Δ-N-LRP6. After 36 hours, F9 cells were stimulated with or without Wnt3a for 30 minutes. Cells were disrupted and fractions (20 mg protein) were subjected to Superdex 200 gel column chromatography. Complexes were fractionated and then analyzed by SDS-PAGE and subjected to immunoblotting. The blots were stained with anti-Dvl3 antibody. Blots were subjected to quantification by calibrated scanner and results displayed are representative of at least two independent experiments.

Dvl3, which can uniquely activate the Lef/Tcf-sensitive pathway in the absence of Wnt3a.

Knockdown of Dvl isoforms blocks formation of supermolecular Dvl3-based complexes in response to Wnt3a

Because overexpression of Dvl1 and Dvl3 promotes formation of supermolecular Dvl3-based complexes, we tested whether or not knockdown of each Dvl isoform would impact the ability of Wnt3a to stimulate formation of these complexes. Knockdown of each Dvl isoforms blocked transcription of Lef/Tcf (data not shown). Knockdown of Dvl3 (as a control) essentially precluded formation of supermolecular complexes in the absence or presence of Wnt3a. Knockdown of Dvl1 did not change the abundance of Dvl3-based complex in the basal state (i.e. without Wnt3a stimulation), but attenuated the ability of Wnt3a to provoke formation of complexes of increased mass (>2.0 MDa). Knockdown of the most abundant isoform Dvl2 (which constitutes >95% of Dvl proteins in F9 cells) severely reduced the abundance of the Dvl3-based complexes in the absence of Wnt3a. Wnt3a failed to stimulate the formation of supermolecular Dvl3-based complexes in cells deficient in Dvl2 (Fig. 6B and supplementary material Fig. S4C). It also did not activate the canonical pathway (data not shown). Clearly Dvl1 and Dvl2 cooperate to catalyze the formation of supermolecular, Dvl3-based complexes in either the absence or presence of Wnt3a.

Supermolecular Dvl3-based complex formation in response to inhibition of GSK3β

Finally, we bypassed proximal Wnt signaling and provoked activation of the Lef/Tcf-sensitive canonical pathway by the chemical inhibition of GSK3β. LiCl effectively abolished GSK3β activity, and stimulated Lef/Tcf-sensitive transcription (Stambolic et al., 1996) (data not shown). Inhibition of GSK3β provoked increased formation of the very large (>2.0 MDa) Dvl3-based complexes (Fig. 6C and supplementary material Fig. S4D). Thus, through targeted activation and disruption of Wnt3a signaling, we show a linkage between the ability to form very large (>2.0 MDa) supermolecular Dvl3-based complexes and functional downstream signaling to the level of activation of Lef/Tcf-sensitive transcription, which represents the hallmark of the Wnt canonical pathway in development.

Analysis of supermolecular Dvl3-based complex formation by fluorescence correlation spectroscopy

We used FCS to probe the apparent size of the Dvl3- and Dvl2-based complexes in live F9 cells. Two populations of eGFP–Dvl3 in unstimulated F9 cells were obtained with diffusion coefficients, 1×10^{-7} cm^2/second and 1.5×10^{-8} cm^2/second. Taking into account the diffusion coefficient of free eGFP in mammalian cells (~1.7×10^{-7} cm^2/second) and the molecular mass of eGFP (27 kDa), we were able to estimate the molecular mass of the two populations of eGFP–Dvl3 in the live F9 cells. If it is assumed that

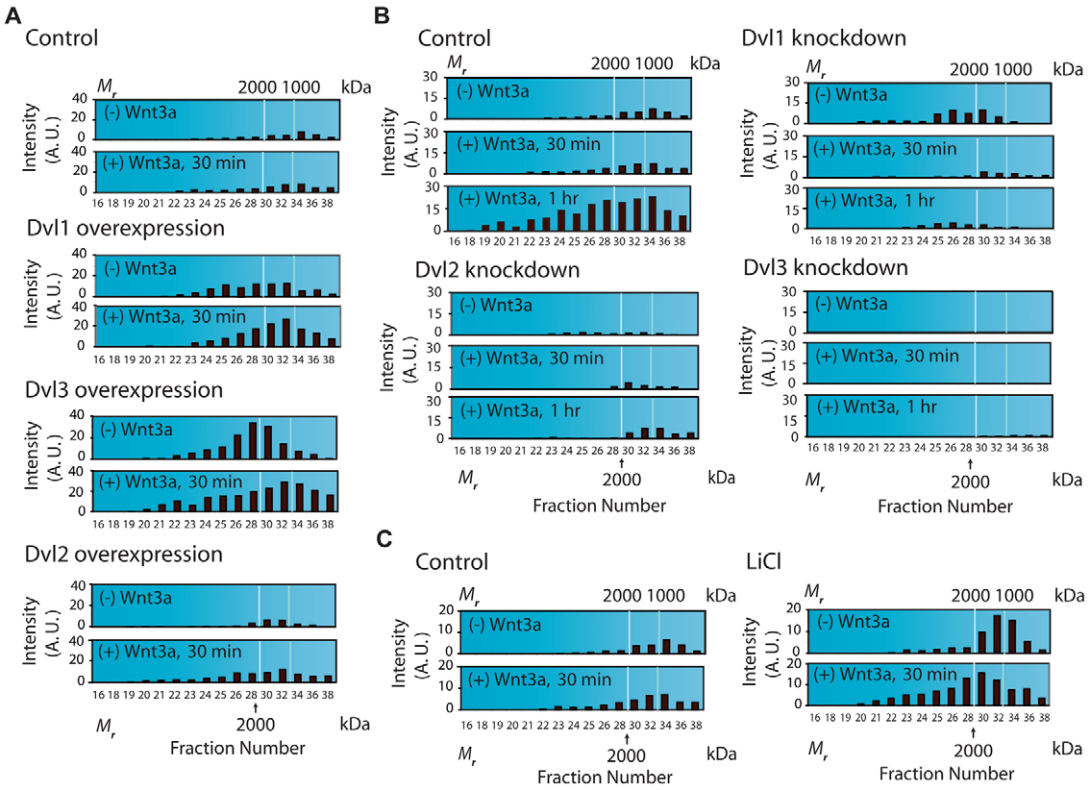

Fig. 6. Mimicking the activation of Wnt pathway provokes formation of supermolecular Dvl3-based complexes. (**A**) Overexpression of Dvl proteins provokes formation of supermolecular Dvl3-based complexes without Wnt3a stimulation. F9 cells were cotransfected with Rfz1 and either GFP- and HA-tagged mouse Dvl1, or Dvl2 or Dvl3. F9 cells were either unstimulated or stimulated with Wnt3a (20 ng/ml) for 30 minutes. Cells were disrupted and lysates were separated by Superdex 200 gel chromatography. Fractions were analyzed by SDS-PAGE. Resolved proteins were immunoblotted with anti-Dvl3 antibody. Blots were quantified and results shown are representative of at least two independent experiments. (**B**) Knockdown of Dvl proteins blocks formation of supermolecular Dvl3-based complexes. F9 cells were transfected with siRNA targeting Dvl1 or Dvl2 or Dvl3, 1 day before transfection with Rfz1. 1 day after transfection, cells were stimulated with or without Wnt3a for the indicated times. Cell extracts were subjected to chromatography on Superdex 200 and fractions were analyzed by SDS-PAGE, immunoblotting and staining with anti-Dvl3 antibody. Blots were quantified and results are displayed. (**C**) Inhibition of GSK3β triggers formation of supermolecular Dvl3-based complexes. F9 cells were either untreated or treated with 30 mM LiCl for 1 hour before Wnt3a. The incubation continued in the presence or absence of 30 mM LiCl. Cell lysates were subjected to gel filtration and fractions were subjected to SDS-PAGE and immunoblotting with anti-Dvl3 antibody. Blots were quantified and results are representative of at least two independent experiments.

both populations are freely diffusing in the cytosol and are spherical, the two populations correspond to Dvl3 dimers (i.e. ~132 kDa) and a population of very large oligomers of ~35 MDa. This large size might include a fraction of Dvl3-based complexes that is membrane associated. Stimulation of the cells with Wnt3a slowed down the diffusion of the larger aggregates, suggesting an increase in molecular mass to ~40 MDa. The diffusion of the smaller oligomers did not change in response to Wnt3a treatment. By sharp contrast, eGFP–Dvl2-based complexes, both before and after stimulation with Wnt3a, displayed a single population with the diffusion coefficient ~1.2×10^{-7} cm^2/second. This mobility corresponds to ~80 kDa, suggesting a Dvl2 monomer. The FCS data agree well with two major observations about the Dvl3-based complexes, which were derived by careful hydrodynamic separation: the complexes are supermolecular and very large (>2 MDa by steric-exclusion chromatography; ~35 MDa by FCS); and the Dvl3-based complex size increases in response to stimulation of the cells by Wnt3a, by both steric-exclusion chromatography and FCS.

Discussion

Dvl proteins are scaffold molecules that are essential for the Wnt canonical β-catenin–Lef/Tcf-sensitive transcriptional response, the planar cell polarity response and the Wnt5a–Frizzled-2–Ca^{2+}–cGMP response (Malbon, 2005; Bikkavilli et al., 2008; Veeman et al., 2003; Angers and Moon, 2009; van Amerongen and Nusse, 2009). Fluorescence microscopy in cells suggests that Dvl proteins undergo dynamic oligomerization associated with activation of Wnt/β-catenin signaling by Wnt3a (Schwarz-Romond et al., 2007a; Schwarz-Romond et al., 2007b). Although the fly displays only a single Dishevelled protein (Dsh), higher-order species express several isoforms of Dvl. Mammalian cells express three isoforms, Dvl1, Dvl2, and Dvl3; each isoform is expressed at varying levels (Sussman et al., 1994; Klingensmith et al., 1996; Gray et al., 2009). Targeted gene disruptions performed in mice (Lijam et al., 1997; Hamblet et al., 2002; Etheridge et al., 2008) as well as knockdown and rescue protocols performed in mouse F9 cells (Lee et al., 2008) demonstrate that mammalian Dvl proteins are not truly 'redundant' with respect to function.

Compelling, albeit indirect, studies suggest that Dvl proteins aggregate and/or oligomerize in response to Wnt stimulation (Schwarz-Romond et al., 2007a). Pull-down studies performed in several cell lines demonstrate that Dvl isoforms interact weakly with each other (Kishida et al., 1999; Lee et al., 2008), through their conserved DIX domain. In mouse F9 cells, we showed that

Dvl2 is by far the most abundant isoform, constituting >95% of the total pool of cellular Dvl proteins. Dvl3, by contrast, constitutes only 1–2% of the pool in mouse or human-derived cells; yet knockdown of the expression of Dvl3 has the most pronounced effect on Wnt signaling (Lee et al., 2008). The aim of the current study was to seek physical evidence for the existence of putative 'aggregates' or 'punctae' of Dvl3-based complexes observed earlier by fluorescence microscopy. These complexes were interrogated physically both in vitro by steric-exclusion chromatography analysis of cell extracts and in vitro by FCS in live cells. The FCS provides data with the upper limit of supermolecular Dvl3-based complexes in live cells, whereas the steric-exclusion chromatography analysis is restricted to a subset that survives the cell lysis and shear forces inherent in the strategy. Thus the apparent inability of steric-exclusion chromatography analysis to resolve large-scale supermolecular Dvl3-based complexes noted by FCS might reflect the shear force overcoming weaker forces of association. Alternatively, dwell time at the cell membrane for supermolecular Dvl3-based complexes might increase the apparent mass of the complexes, as analyzed by FCS. Irrespective of this, both steric-exclusion chromatography and FCS detect supermolecular Dvl3-based complexes whose mass is markedly increased when cells are stimulated with Wnt3a.

The in vitro analysis of cell extracts clearly identified Dvl3-based complexes that range in size from apparent dimers (130–200 kDa) to very large supermolecular complexes of 0.5 to ~2 MDa. Other signaling molecules that form SDS-resistant oligomers include: enzymes such as Na^+/K^+-ATPase and eNOS; the GPCR, rhodopsin (Soulie et al., 1996); and members of the AKAP family, especially AKAP12. AKAP12 requires 8M urea for dissociation of oligomers (Tao et al., 2003). Many membrane-associating proteins form SDS-resistant complexes (Sagne et al., 1996). Dvl3-based nuclear complexes, for comparison of scale (i.e. complexes that include Tcf4, c-Jun, β-catenin, and other Dvl-interacting proteins) are ~2.0 MDa (Gan et al., 2008). Another estimate of the apparent molecular mass of such Dvl3-based complexes can be calculated by simple compilation of the predicted masses of Dvl-interacting proteins posited in 'The Wnt home page' (http://www.stanford.edu/~rnusse/ wntwindow.html). Assuming each Dvl-interacting protein included in the list is represented in molar equivalent, the calculated mass for such a hypothetical complex is ~2.0 MDa. The FCS analysis benefits from providing information on the size of Dvl3-based complexes probed in live F9 cells as a real-time measurement. eGFP-tagged Dvl3 was tracked and the molecular mass calculated from the diffusion coefficients. Two populations of Dvl3-based complexes were readily apparent. The smaller (~132 kDa) would be consistent with Dvl3 dimers or Dvl3 in combination with a protein(s) with an aggregate mass equivalent to Dvl3. The second major population displayed a diffusion coefficient from which a mass of ~35 MDa was calculated. The difference in apparent molecular mass between Dvl3-based complexes deduced in cell extracts by hydrodynamics versus measurements in live cells by FCS is of interest. Some of the difference might reflect the extent to which these complexes deviate from being truly spherical in nature. The higher-order supermolecular complexes with Dvl3 of ~35 MDa might represent oligomers composed of smaller 'building blocks' of the 2 MDa species observed in vitro. The hydrodynamic stress of such high-performance separations might well disrupt the larger, weakly interacting oligomers. Alternatively, the 35 MDa Dvl3-based species might represent the 2 MDa complexes alone (or in oligomers) docking transiently with the cell membrane or structural elements such as the cytoskeleton. The Dvl2-based complexes, in sharp contrast to the Dvl3-based ones, displayed diffusion coefficients from which a mass of ~80 kDa could be calculated. It must be kept in mind that the relative abundance of Dvl2 is 50-fold greater than that of Dvl3, so an over-representation of monomeric Dvl2 might be anticipated in FCS.

To begin to address the functional significance of the supermolecular Dvl3-based complexes, we investigated whether the apparent mass of these complexes was regulated by Wnt3a, in vitro and in vivo using FCS. Wnt3a was observed to provoke a dramatic shift in the apparent mass of the Dvl3-based complexes to populations with sharply larger masses (>2.0 MDa). We established the presence of several key Dvl-interacting proteins in these very large, supermolecular Dvl3-based complexes (e.g. Dvl1, Dvl2, Dvl3, GSK3β and Axin). The formation of these very large complexes in response to Wnt3a was found to be time-dependent and dynamic in character, i.e. it displayed reversibility. Activation of Wnt/β-catenin signaling examined earlier by fluorescence microscopy suggested the existence of a higher order of assembly (i.e. supermolecular 'punctate' structures containing Dvl2, Axin and other proteins) whose size cannot be accounted by simple Dvl dimerization (Schwarz-Romond et al., 2007a). Likewise, it has been suggested that Dvl-based 'punctate' structures are dynamic protein assemblies, not cytoplasmic vesicles (Schwarz-Romond, 2005); we found no evidence to support liposome-dependent association in our studies. Previous in situ BRET analysis also demonstrated the association of Dvl and Axin upon Wnt stimulation (Yokoyama et al., 2007).

To probe the functional meaning of supermolecular assemblies of Dvl3 further, we asked whether mimicking Wnt3a action (in the absence of Wnt3a) would provoke Dvl3-based supermolecular complex formation. We followed the Lef/Tcf-sensitive transcriptional activation and probed complex formation of Dvl3 using steric-exclusion analysis (Table 1). Expression of the constitutively active Δ-N-LRP6, overexpression of either Dvl1 or Dlv3, and chemical inhibition of GSK3β each stimulated Lef/Tcf-sensitive transcription in the absence of Wnt3a; each of these experimental interventions also stimulated the formation of higher-order Dvl3-based supermolecular complexes in the absence of Wnt3a. Conversely, DKK1 treatment, expression of the dominant-interfering Δ-C-LRP6 and knockdown of Dvl3 all blocked the ability of Wnt3a to stimulate the canonical pathway, while blocking the formation of higher order, Dvl3-based supermolecular complexes. These data are consistent with the notion that the

Table 1. Summary of Wnt activation and formation of Dvl3-based complexes

	Wnt3a (–)		Wnt3a (+)	
	Dvl3-based complexes	Lef/Tcf transcription	Dvl3-based complexes	Lef/Tcf transcription
Control	–	–	+	+
Δ-N-LRP6	+	+	+	+
Δ-C-LRP6	–	–	–	–
LiCl	+	+	+	+
Dvl1 overexpression	+	+	+	+
Dvl2 overexpression	±	+	+	+
Dvl3 overexpression	+	+	+	+
DKK1	–	–	–	–
Dvl1 knockdown	+	–	±	–
Dvl2 knockdown	±	–	±	–
Dvl3 knockdown	–	–	–	–

ability of Wnt3a to propagate signaling in the canonical pathway requires the concurrent ability to assemble higher-order Dvl3-based supermolecular complexes (Table 1). We also note that knockdown of either Dvl1 or Dvl3 alters the abundance of GSK3β as well as the migration of GSK3β in response to Wnt3a. Thus, we establish the first physical identification and sizing of very large, dynamic supermolecular Dvl-based complexes both in untreated and Wnt3a-stimulated cells. Manipulations that provoke the formation of these Dvl3-based complexes also provoke activation of the Wnt/β-catenin canonical pathway. Analysis of the dynamic formation of higher-order Dvl3-based supermolecular complexes can be achieved in vitro through steric-exclusion chromatography and in vivo by FCS in live cells.

Materials and Methods

Materials

The following reagents were purchased from the indicated commercial supplier(s): anti-Dvl1, anti-Dvl2, anti-Dvl3, anti-Axin and anti-LRP6 antibodies from Santa Cruz Biotechnology (Santa Cruz, CA); anti-GSK3β and anti-Dvl3 antibodies from Cell Signaling (Danvers, MA); Immobilon membrane from Millipore (Bedford, MA); purified, biologically active Wnt3a, purified DKK1 and anti-Axin antibody from R and D Systems (Minneapolis, MN). Plasmids of wild type-LRP6, Δ-N-LRP6 and Δ-C-LRP6 were kind gifts from K. Tamai (Case Western University, Cleveland, OH).

Cell culture and transfection

The mouse F9 teratocarcinoma cells (F9) cells, transfected with pcDNA3 expression vector harboring rat Frizzled-1 (Rfz1), were grown in Dulbecco's modified Eagle's medium (DMEM) as described previously (Yokoyama and Malbon, 2007). Cells were transfected transiently with an expression vector (pCDNA3) harboring the rat Frizzled-1 (Rfz1) using lipofectamine (Invitrogen, Carlsbad, CA), according to the commercial instructions. For the overexpression study, green fluorescence protein (GFP)- and hemagglutinin (HA)-tagged mouse Dvl isoforms were transiently transfected to F9 cells with Rfz1 48 hours before Wnt3a stimulation.

Knock down of Dvls by siRNA

siRNA sequences designed to suppress Dvl proteins are as follows: siRNA sequences targeting Dvl1, CCAGGAUAUUGGCUUGACAtt and UGUCAAGCC-AAUAUCCUGGtg; siRNA sequences targeting Dvl2, GGAAGAGAUCUCC-GAUGACtt and GUCAUCGGAGAUCUCUUCCtt; siRNA sequences targeting Dvl3, GGAAGAGAUCUCGGACGACtt and GUCGUCCGAGAUCUCUUCCtt. After 1 day of treatment with siRNA targeting either Dvl1, or Dvl2, or Dvl3, cells were transfected with an expression vector harboring Rfz1. On the following day, F9 cells were stimulated with or without Wnt3a for indicated time.

Separation of Dvl2 complexes and protein extraction from gels

F9 cells were lysed with RIPA buffer (50 mM Tris-HCl, pH 7.2, 150 mM NaCl, 5 mM EDTA, 2 mM sodium orthovanadate, 0.25% sodium deoxycholate, and 0.05% SDS). Cell lysates (40 mg protein) were subjected to immunoprecipitation with Dvl2 antibody overnight. Bound proteins were analyzed by SDS-PAGE and stained with Coomassie Brilliant Blue. Bands were excised from the gel, cut into small pieces and, crushed gel pieces were incubated with buffer (50 mM Tris-HCl, pH 7.5, 150 mM NaCl, and 0.1 mM EDTA) at 30°C overnight with rocking. After centrifugation, the supernatant was used for analysis.

Separation of Dvl-based supermolecular complexes by steric-exclusion chromatography

F9 cells coexpressing Rfz1 were suspended in ice-cold buffer (20 mM Tris-HCl pH 8.0, 0.2 M NaCl, 1% NP-40, 1 mM PMSF, 10 μg/ml leupeptin, and 10 μg/ml aprotinin) and disrupted by repeated passage through a 23-gauge needle, and then centrifuged to remove unbroken cells, nuclei and mitochondria. Supernatants were filtered (0.45 μm) and diluted with buffer without detergent. 20 mg proteins were applied to the Superdex 200 gel filtration column (HiLoad Superdex^{TM} 200 prep grade 26/60, fast-performance liquid chromatography system AKTA, GE Healthcare), which was pre-equilibrated with 20 mM Tris-HCl, pH 8.0, 0.2 M NaCl, and 10% glycerol. 0.9 ml fractions were collected. Each fraction was analyzed by SDS-PAGE and western immunoblotting. Protein concentration was determined using the Bradford assay. For more precise analysis of MDa complexes, cell lysates were separated by Sephacryl S-400 gel filtration column (HiPrep Sephacryl S-400 High resolution column, fast-performance AKTA liquid chromatography, GE Healthcare).

Fluorescence correlation spectroscopy of Dvl3-based complexes in live cells

FCS measurements were performed on a Zeiss LSM 510 Meta/Confocor 2 apparatus (Jena, Germany) fitted with a 40× NA 1.2 C-Apochromat water-immersion objective. We used standard configurations and minimal laser powers to avoid photobleaching. The pinholes were adjusted at least daily and the detection volume was calibrated by measuring the diffusion of Rhodamine (Rh6G, D=3×10^{-6} cm^2/second) in water (Hess et al., 2002). All measurements were performed at room temperature. We excited eGFP with the 488 nm line of argon ion laser and collected emission spectra through a 505 LP filter. We used software provided by Zeiss to fit the autocorrelation curves to the model equation for free Brownian diffusion commonly used in FCS (Schwille et al., 1999):

$$G(\tau) = \frac{1}{N} \cdot \sum_i \frac{Y_i}{1 + \frac{\tau}{\tau_{d,i}}} \quad (1)$$

where N is the number of molecules in the detection volume, Y_i is the fraction of molecules diffusing with diffusion coefficient D_i producing residence times $\tau_{d,i}$. We calculated the diffusion coefficient D from the Einstein relation, $D=r^2/4\tau_d$.

To estimate the approximate molecular mass of diffusing complexes we assumed that the complexes are spherical and used the following equation to determine the hydrodynamic radius (Lakowicz, 2006): $D=kT/6\pi\eta R$, where, k is the Boltzmann constant, T is the temperature, η is the viscosity of the solvent, and R is the hydrodynamic radius. Molecular mass is related to R by following equation:

$$V = MW\bar{v} = \frac{4}{3}\pi R^3 \quad (2)$$

where, V is volume and $\bar{v}$ is specific gravity. To account for the viscosity of the cells we used values obtained for GFP in cells, D=1.7×10^{-7} cm^2/second and the molecular mass is 27 kDa (Brock et al., 1999).

Immunoblotting and immunoprecipitation

Proteins were analyzed by SDS-PAGE and immunoblotting (Yokoyama et al., 2007). Immune complexes were made visible using a horseradish-peroxidase-conjugated, secondary antibody in tandem with ECL chemiluminescence. For immunoprecipitation experiments, fractions were immunoprecipitated with primary antibody overnight at 4°C. After beads were washed with phosphate-buffered saline containing 0.5% NP-40, bound proteins were eluted by SDS-sample buffer and then analyzed by SDS-PAGE and immunoblotting.

Quantification of proteins

Immunoreactive bands were scanned by calibrated Umax 1000 scanner equipped with SilverFast software (LaserSoft Imaging, Longboat Key, FL). The bands were quantified by using Aida software (Raytest, Germany).

We thank the members of the laboratory for careful discussions and critical review of the manuscript. This work was supported generously by United States Public Health Services grants (to C.C.M.) from the National Institute of Diabetes, Digestive and Kidney Diseases, NIH and (to H.-y.W.) from the National Institute of General Medical Sciences, NIH. The author(s) declare no conflict of interest and that they have no competing interests, financial or otherwise. Deposited in PMC for immediate release. This article is freely available online from the date of publication.

Supplementary material available online at
http://jcs.biologists.org/cgi/content/full/123/21/3693/DC1

References

Angers, S. and Moon, R. T. (2009). Proximal events in Wnt signal transduction. *Nat. Rev. Mol. Cell Biol.* **10**, 468-477.

Axelrod, J. D., Miller, J. R., Shulman, J. M., Moon, R. T. and Perrimon, N. (1998). Differential recruitment of Dishevelled provides signaling specificity in the planar cell polarity and Wingless signaling pathways. *Genes Dev.* **12**, 2610-2622.

Bikkavilli, R. K., Feigin, M. E. and Malbon, C. C. (2008). G alpha o mediates WNT-JNK signaling through dishevelled 1 and 3, RhoA family members, and MEKK 1 and 4 in mammalian cells. *J. Cell Sci.* **121**, 234-245.

Bilic, J., Huang, Y. L., Davidson, G., Zimmermann, T., Cruciat, C. M., Bienz, M. and Niehrs, C. (2007). Wnt induces LRP6 signalosomes and promotes dishevelled-dependent LRP6 phosphorylation. *Science* **316**, 1619-1622.

Brock, R., Vamosi, G., Vereb, G. and Jovin, T. M. (1999). Rapid characterization of green fluorescent protein fusion proteins on the molecular and cellular level by fluorescence correlation microscopy. *Proc. Natl. Acad. Sci. USA* **96**, 10123-10128.

Clevers, H. (2006). Wnt/beta-catenin signaling in development and disease. *Cell* **127**, 469-480.

Etheridge, S. L., Ray, S., Li, S., Hamblet, N. S., Lijam, N., Tsang, M., Greer, J., Kardos, N., Wang, J. and Sussman, D. J. et al. (2008). Murine dishevelled 3 functions in redundant pathways with dishevelled 1 and 2 in normal cardiac outflow tract, cochlea, and neural tube development. *PLoS Genet.* **4**, e1000259.

Gan, X. Q., Wang, J. Y., Xi, Y., Wu, Z. L., Li, Y. P. and Li, L. (2008). Nuclear Dvl, c-Jun, beta-catenin, and TCF form a complex leading to stabilization of beta-catenin-TCF interaction. *J. Cell Biol.* **180**, 1087-1100.

Glass, D. A., 2nd and Karsenty, G. (2006). Molecular bases of the regulation of bone remodeling by the canonical Wnt signaling pathway. *Curr. Top. Dev. Biol.* **73**, 43-84.

Gray, R. S., Bayly, R. D., Green, S. A., Agarwala, S., Lowe, C. J. and Wallingford, J. B. (2009). Diversification of the expression patterns and developmental functions of the dishevelled gene family during chordate evolution. *Dev. Dyn.* **238**, 2044-2057.

Hamblet, N. S., Lijam, N., Ruiz-Lozano, P., Wang, J., Yang, Y., Luo, Z., Mei, L., Chien, K. R., Sussman, D. J. and Wynshaw-Boris, A. (2002). Dishevelled 2 is essential for cardiac outflow tract development, somite segmentation and neural tube closure. *Development* **129**, 5827-5838.

Hart, M. J., de los Santos, R., Albert, I. N., Rubinfeld, B. and Polakis, P. (1998). Downregulation of beta-catenin by human Axin and its association with the APC tumor suppressor, beta-catenin and GSK3 beta. *Curr. Biol.* **8**, 573-581.

He, X., Semenov, M., Tamai, K. and Zeng, X. (2004). LDL receptor-related proteins 5 and 6 in Wnt/beta-catenin signaling: arrows point the way. *Development* **131**, 1663-1677.

Hess, S. T., Huang, S., Heikal, A. A. and Webb, W. W. (2002). Biological and chemical applications of fluorescence correlation spectroscopy: a review. *Biochemistry* **41**, 697-705.

Katanaev, V. L., Ponzielli, R., Semeriva, M. and Tomlinson, A. (2005). Trimeric G protein-dependent frizzled signaling in Drosophila. *Cell* **120**, 111-122.

Kishida, S., Yamamoto, H., Ikeda, S., Kishida, M., Sakamoto, I., Koyama, S. and Kikuchi, A. (1998). Axin, a negative regulator of the wnt signaling pathway, directly interacts with adenomatous polyposis coli and regulates the stabilization of beta-catenin. *J. Biol. Chem.* **273**, 10823-10826.

Kishida, S., Yamamoto, H., Hino, S., Ikeda, S., Kishida, M. and Kikuchi, A. (1999). DIX domains of Dvl and axin are necessary for protein interactions and their ability to regulate beta-catenin stability. *Mol. Cell. Biol.* **19**, 4414-4422.

Klingensmith, J., Yang, Y., Axelrod, J. D., Beier, D. R., Perrimon, N. and Sussman, D. J. (1996). Conservation of dishevelled structure and function between flies and mice: isolation and characterization of Dvl2. *Mech. Dev.* **58**, 15-26.

Lakowicz, J. R. (2006). *Principles of Fluorescence Spectroscopy*, 3rd edn. New York: Springer.

Lee, Y. N., Gao, Y. and Wang, H. Y. (2008). Differential mediation of the Wnt canonical pathway by mammalian Dishevelleds-1, -2, and -3. *Cell Signal.* **20**, 443-452.

Lijam, N., Paylor, R., McDonald, M. P., Crawley, J. N., Deng, C. X., Herrup, K., Stevens, K. E., Maccaferri, G., McBain, C. J., Sussman, D. J. et al. (1997). Social interaction and sensorimotor gating abnormalities in mice lacking Dvl1. *Cell* **90**, 895-905.

Liu, T., DeCostanzo, A. J., Liu, X., Wang, H., Hallagan, S., Moon, R. T. and Malbon, C. C. (2001). G protein signaling from activated rat frizzled-1 to the beta-catenin-Lef-Tcf pathway. *Science* **292**, 1718-1722.

Malbon, C. C. (2005). G proteins in development. *Nat. Rev. Mol. Cell Biol.* **6**, 689-701.

Miller, J. R., Rowning, B. A., Larabell, C. A., Yang-Snyder, J. A., Bates, R. L. and Moon, R. T. (1999). Establishment of the dorsal-ventral axis in Xenopus embryos coincides with the dorsal enrichment of dishevelled that is dependent on cortical rotation. *J. Cell Biol.* **146**, 427-437.

Nusse, R. (2001). Developmental biology. Making head or tail of Dickkopf. *Nature* **411**, 255-256.

Nusse, R. (2005). Wnt signaling in disease and in development. *Cell Res.* **15**, 28-32.

Rothbacher, U., Laurent, M. N., Deardorff, M. A., Klein, P. S., Cho, K. W. and Fraser, S. E. (2000). Dishevelled phosphorylation, subcellular localization and multimerization regulate its role in early embryogenesis. *EMBO J.* **19**, 1010-1022.

Sagne, C., Isambert, M. F., Henry, J. P. and Gasnier, B. (1996). SDS-resistant aggregation of membrane proteins: application to the purification of the vesicular monoamine transporter. *Biochem. J.* **316**, 825-831.

Schwarz-Romond, T., Fiedler, M., Shibata, N., Butler, P. J., Kikuchi, A., Higuchi, Y. and Bienz, M. (2007a). The DIX domain of Dishevelled confers Wnt signaling by dynamic polymerization. *Nat. Struct. Mol. Biol.* **14**, 484-492.

Schwarz-Romond, T., Merrifield, C., Nichols, B. J. and Bienz, M. (2005). The Wnt signalling effector Dishevelled forms dynamic protein assemblies rather than stable associations with cytoplasmic vesicles. *J. Cell Sci.* **118**, 5269-5277.

Schwarz-Romond, T., Metcalfe, C. and Bienz, M. (2007b). Dynamic recruitment of axin by Dishevelled protein assemblies. *J. Cell Sci.* **120**, 2402-2412.

Schwille, P., Haupts, U., Maiti, S. and Webb, W. W. (1999). Molecular dynamics in living cells observed by fluorescence correlation spectroscopy with one- and two-photon excitation. *Biophys. J.* **77**, 2251-2265.

Soulie, S., Moller, J. V., Falson, P. and le Maire, M. (1996). Urea reduces the aggregation of membrane proteins on sodium dodecyl sulfate-polyacrylamide gel electrophoresis. *Anal. Biochem.* **236**, 363-364.

Stambolic, V., Ruel, L. and Woodgett, J. R. (1996). Lithium inhibits glycogen synthase kinase-3 activity and mimics wingless signalling in intact cells. *Curr. Biol.* **6**, 1664-1668.

Sussman, D. J., Klingensmith, J., Salinas, P., Adams, P. S., Nusse, R. and Perrimon, N. (1994). Isolation and characterization of a mouse homolog of the Drosophila segment polarity gene dishevelled. *Dev. Biol.* **166**, 73-86.

Tamai, K., Zeng, X., Liu, C., Zhang, X., Harada, Y., Chang, Z. and He, X. (2004). A mechanism for Wnt coreceptor activation. *Mol. Cell* **13**, 149-156.

Tao, J., Wang, H. Y. and Malbon, C. C. (2003). Protein kinase A regulates AKAP250 (gravin) scaffold binding to the beta2-adrenergic receptor. *EMBO J.* **22**, 6419-6429.

van Amerongen, R. and Nusse, R. (2009). Towards an integrated view of Wnt signaling in development. *Development* **136**, 3205-3214.

Veeman, M. T., Axelrod, J. D. and Moon, R. T. (2003). A second canon. Functions and mechanisms of beta-catenin-independent Wnt signaling. *Dev. Cell* **5**, 367-377.

Wallingford, J. B. and Habas, R. (2005). The developmental biology of Dishevelled: an enigmatic protein governing cell fate and cell polarity. *Development* **132**, 4421-4436.

Wang, J. and Wynshaw-Boris, A. (2004). The canonical Wnt pathway in early mammalian embryogenesis and stem cell maintenance/differentiation. *Curr. Opin. Genet. Dev.* **14**, 533-539.

Wharton, K. A., Jr (2003). Runnin' with the Dvl: proteins that associate with Dsh/Dvl and their significance to Wnt signal transduction. *Dev. Biol.* **253**, 1-17.

Willert, K., Brown, J. D., Danenberg, E., Duncan, A. W., Weissman, I. L., Reya, T., Yates, J. R., 3rd and Nusse, R. (2003). Wnt proteins are lipid-modified and can act as stem cell growth factors. *Nature* **423**, 448-452.

Wodarz, A. and Nusse, R. (1998). Mechanisms of Wnt signaling in development. *Annu. Rev. Cell Dev. Biol.* **14**, 59-88.

Wong, H. C., Bourdelas, A., Krauss, A., Lee, H. J., Shao, Y., Wu, D., Mlodzik, M., Shi, D. L. and Zheng, J. (2003). Direct binding of the PDZ domain of Dishevelled to a conserved internal sequence in the C-terminal region of Frizzled. *Mol. Cell* **12**, 1251-1260.

Yamamoto, H., Komekado, H. and Kikuchi, A. (2006). Caveolin is necessary for Wnt-3a-dependent internalization of LRP6 and accumulation of beta-catenin. *Dev. Cell* **11**, 213-223.

Yokoyama, N. and Malbon, C. C. (2007). Phosphoprotein phosphatase-2A docks to Dishevelled and counterregulates Wnt3a/beta-catenin signaling. *J. Mol. Signal.* **2**, 12.

Yokoyama, N., Yin, D. and Malbon, C. C. (2007). Abundance, complexation, and trafficking of Wnt/beta-catenin signaling elements in response to Wnt3a. *J. Mol. Signal.* **2**, 11.

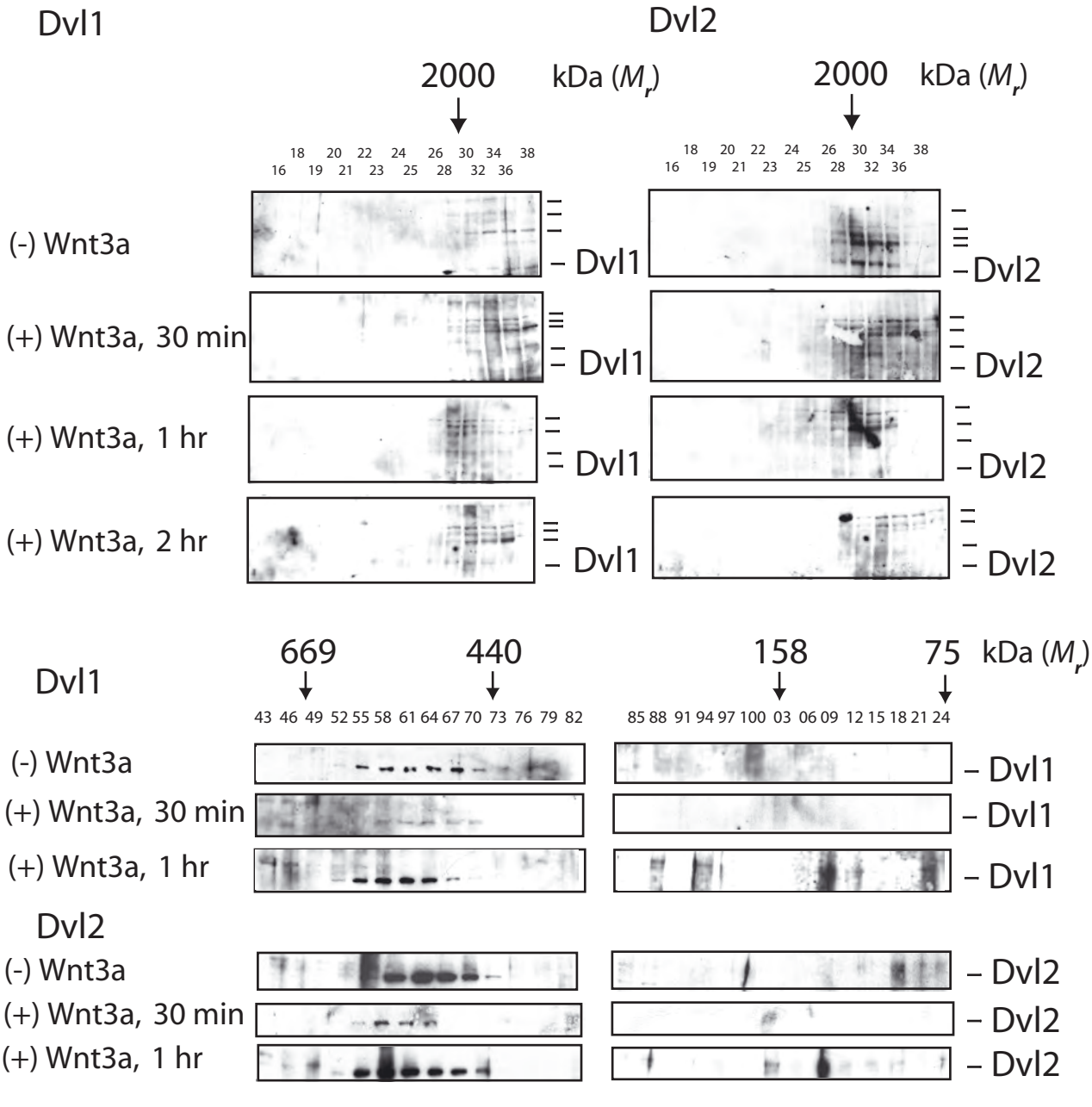
Dvl1
Dvl2
2000
kDa (M_r)
2000
kDa (M_r)
18 20 22 24 26 30 34 38
16 19 21 23 25 28 32 36
18 20 22 24 26 30 34 38
16 19 21 23 25 28 32 36
(-) Wnt3a
(+) Wnt3a, 30 min
(+) Wnt3a, 1 hr
(+) Wnt3a, 2 hr
Dvl1
Dvl2
669
440
158
75
kDa (M_r)
43 46 49 52 55 58 61 64 67 70 73 76 79 82
85 88 91 94 97 100 03 06 09 12 15 18 21 24
(-) Wnt3a
(+) Wnt3a, 30 min
(+) Wnt3a, 1 hr
Dvl1
(-) Wnt3a
(+) Wnt3a, 30 min
(+) Wnt3a, 1 hr
Dvl2

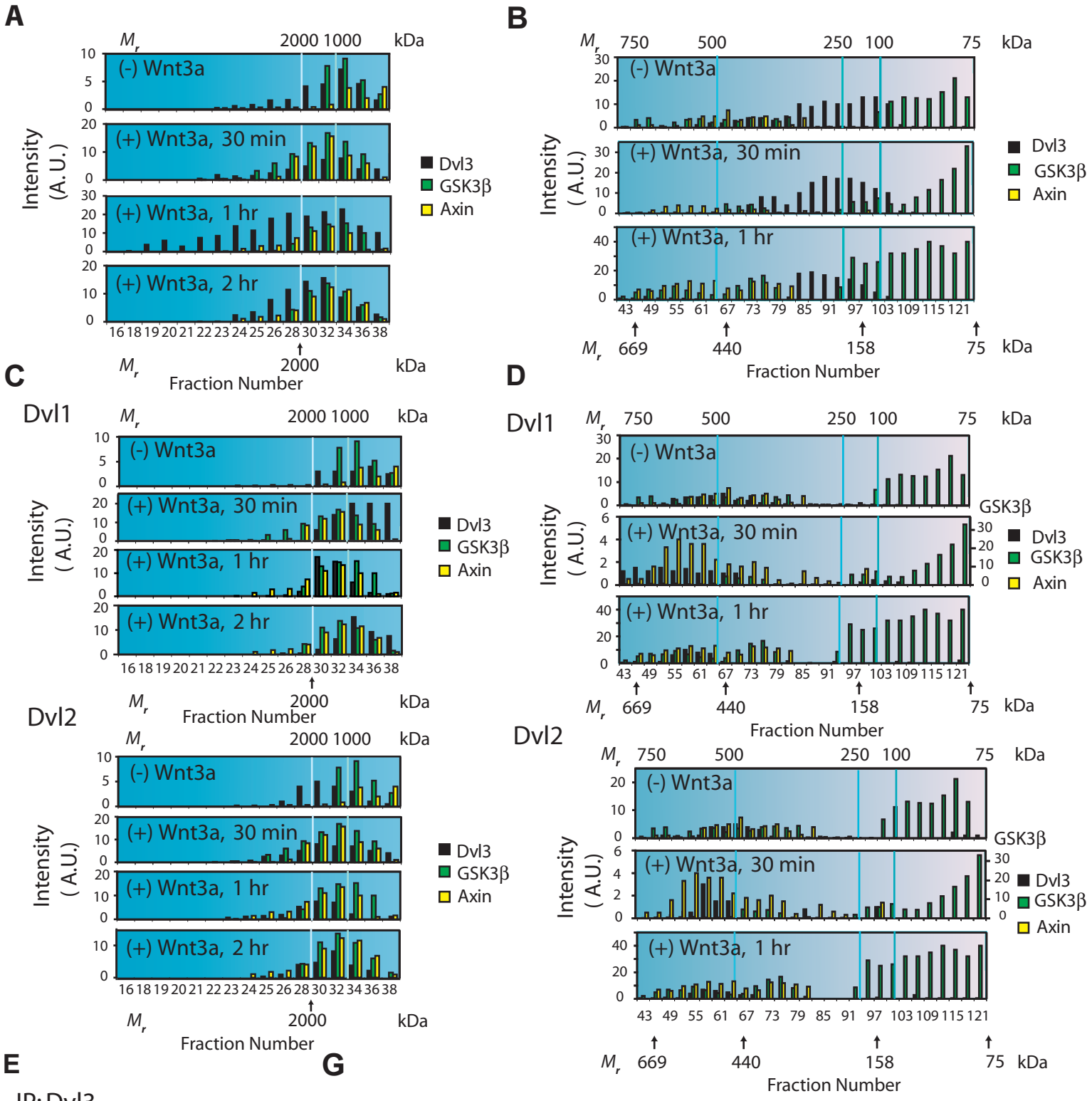
A
B
C
D
E
F
G
H
Dvl1
Dvl2
IP: Dvl3
Blot: LRP6
HEK cell
Silver-stained protein
(-) Wnt3a
(+) Wnt3a, 30 min
(+) Wnt3a, 1 hr
(+) Wnt3a, 2 hr
Dvl3
GSK3β
Axin
Intensity (A.U.)
Fraction Number
kDa

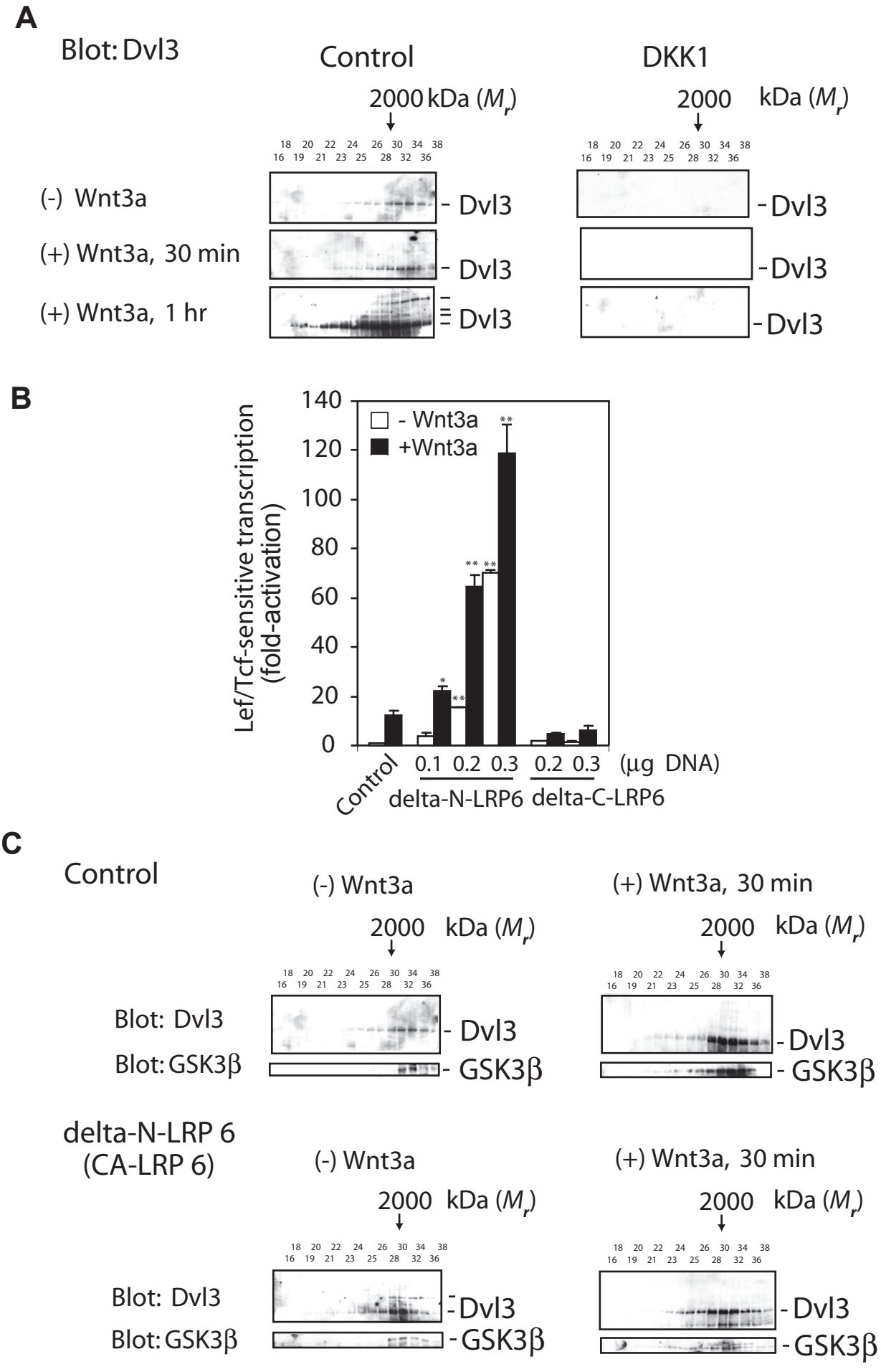
A
Blot: Dvl3
Control
DKK1
2000 kDa (M_r)
2000 kDa (M_r)
18 20 22 24 26 30 34 38
16 19 21 23 25 28 32 36
(-) Wnt3a
(+) Wnt3a, 30 min
(+) Wnt3a, 1 hr
- Dvl3
- Dvl3
- Dvl3
- Dvl3
- Dvl3
- Dvl3
B
Lef/Tcf-sensitive transcription (fold-activation)
140
120
100
80
60
40
20
0
- Wnt3a
+Wnt3a
**
**
**
*
**
Control
0.1 0.2 0.3
0.2 0.3
(µg DNA)
delta-N-LRP6
delta-C-LRP6
C
Control
(-) Wnt3a
(+) Wnt3a, 30 min
2000 kDa (M_r)
2000 kDa (M_r)
18 20 22 24 26 30 34 38
16 19 21 23 25 28 32 36
Blot: Dvl3
Blot: GSK3β
- Dvl3
- GSK3β
- Dvl3
- GSK3β
delta-N-LRP 6
(CA-LRP 6)
(-) Wnt3a
(+) Wnt3a, 30 min
2000 kDa (M_r)
2000 kDa (M_r)
18 20 22 24 26 30 34 38
16 19 21 23 25 28 32 36
Blot: Dvl3
Blot: GSK3β
- Dvl3
- GSK3β
- Dvl3
- GSK3β

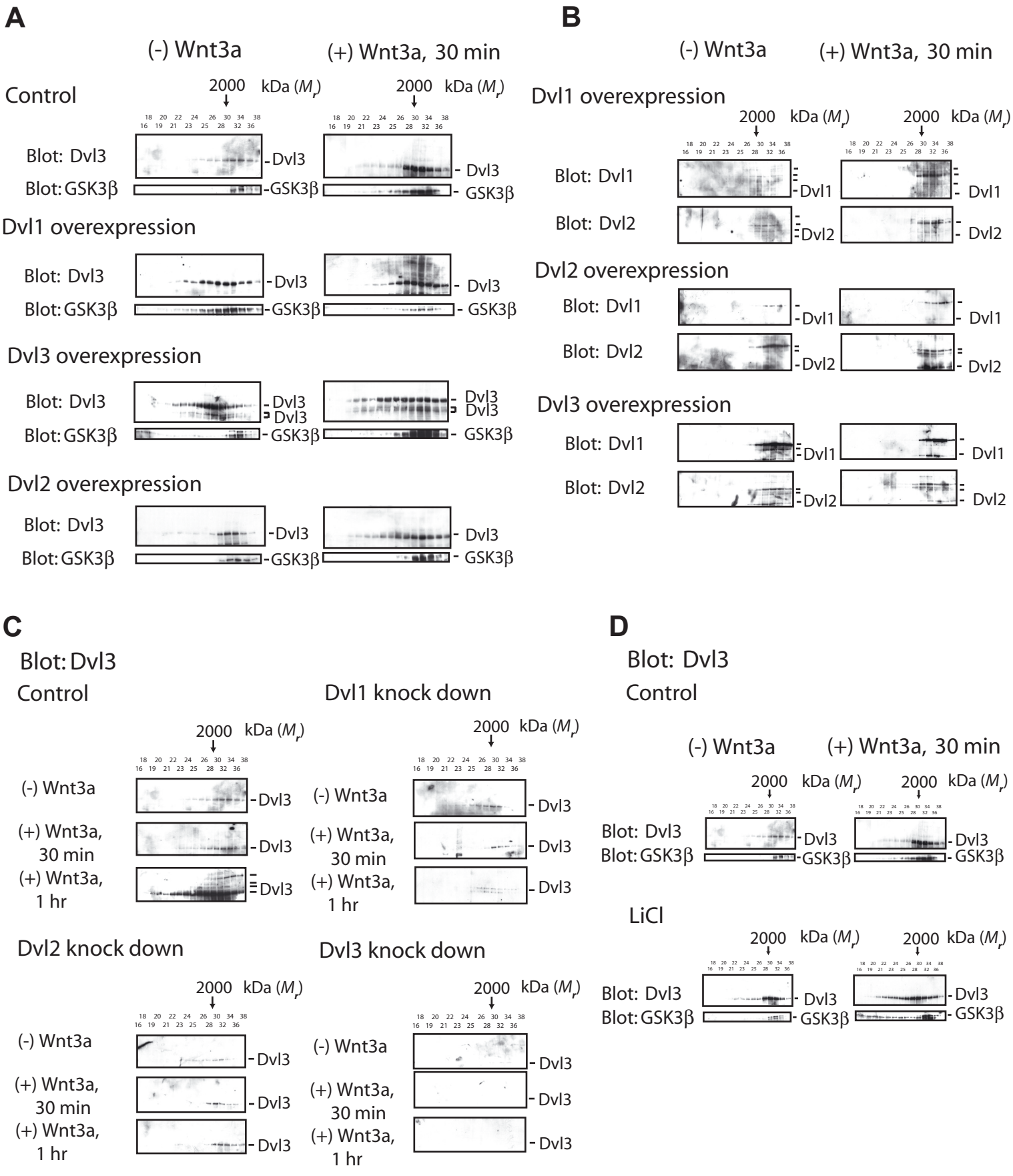
A
(-) Wnt3a
(+) Wnt3a, 30 min
Control
2000 kDa (M_r)
Blot: Dvl3
Blot: GSK3β
Dvl3
GSK3β
Dvl1 overexpression
Dvl3 overexpression
Dvl2 overexpression
B
(-) Wnt3a
(+) Wnt3a, 30 min
Dvl1 overexpression
2000 kDa (M_r)
Blot: Dvl1
Blot: Dvl2
Dvl1
Dvl2
Dvl2 overexpression
Dvl3 overexpression
C
Blot: Dvl3
Control
Dvl1 knock down
Dvl2 knock down
Dvl3 knock down
(-) Wnt3a
(+) Wnt3a, 30 min
(+) Wnt3a, 1 hr
2000 kDa (M_r)
Dvl3
D
Blot: Dvl3
Control
(-) Wnt3a
(+) Wnt3a, 30 min
2000 kDa (M_r)
Blot: Dvl3
Blot: GSK3β
Dvl3
GSK3β
LiCl